Designed guanidinium-rich amphipathic oligocarbonate molecular transporters complex, deliver and release siRNA in cells

Erika I. Geihe[a,b,1], Christina B. Cooley[a,b,1], Jeff R. Simon[a], Matthew K. Kiesewetter[a], Justin A. Edward[a], Robyn P. Hickerson[c], Roger L. Kaspar[c,d], James L. Hedrick[e], Robert M. Waymouth[a], and Paul A. Wender[a,b,2]

[a]Department of Chemistry, Stanford University, Stanford, CA 94305; [b]Department of Chemical and Systems Biology, Stanford University, Stanford, CA 94305; [c]TransDerm Inc., 2161 Delaware Avenue, Suite D, Santa Cruz, CA 95060; [d]Department of Pediatrics, Stanford University, Stanford, CA 94305; and [e]IBM Almaden Research Center, 650 Harry Road, San Jose, CA 95120

The polyanionic nature of oligonucleotides and their enzymatic degradation present challenges for the use of siRNA in research and therapy; among the most notable of these is clinically relevant delivery into cells. To address this problem, we designed and synthesized the first members of a new class of guanidinium-rich amphipathic oligocarbonates that noncovalently complex, deliver, and release siRNA in cells, resulting in robust knockdown of target protein synthesis in vitro as determined using a dual-reporter system. The organocatalytic oligomerization used to synthesize these co-oligomers is step-economical and broadly tunable, affording an exceptionally quick strategy to explore chemical space for optimal siRNA delivery in varied applications. The speed and versatility of this approach and the biodegradability of the designed agents make this an attractive strategy for biological tool development, imaging, diagnostics, and therapeutic applications.

amphipathic co-oligomers | nanoparticles | oligonucleotide delivery | biodegradable oligomers | organocatalysis

RNA interference (RNAi) is an emerging technology that is revolutionizing many strategic approaches to biochemical pathway analysis, drug discovery, and therapy (1–6). As part of the RNAi pathway, small interfering RNAs (siRNAs) induce post-transcriptional, sequence-specific gene silencing utilizing endogenous intracellular machinery to selectively suppress gene expression and, thereby, reduce target protein synthesis (7). The net effect is equivalent to protein inhibition without the use of small molecule inhibitors. The specificity of RNAi also allows one to make inhibitors against previously undruggable targets. Both the ubiquity of the RNAi pathway within the body and the ease with which siRNA can be used to suppress a specific target of interest have made siRNAs a promising class of molecules for the treatment of cancer, viral infections, ocular disorders, and genetic diseases (5). In 2004, the first siRNA-based therapy entered Phase 1 clinical trials (4). Since then, several other RNAi-based therapies have reached clinical evaluation for a number of indications including cancer, viral infections, and genetic skin disorders (5, 8, 9). Notwithstanding this progress, formidable challenges remain for the application of RNAi technology in basic research and therapy, the most fundamental of which is delivery of siRNA across biological barriers.

The siRNAs are double-stranded RNA molecules typically consisting of a 19–23 base-paired region with two 3′ overhanging nucleotides. It is polyanionic, polar, and large (ca. 13 kDa), compared to small molecule therapeutics. These physical properties suppress or prevent its unassisted passage through nonpolar membranes and, thus, its access to the intracellular RNA-induced silencing complex (RISC) components required for target protein knockdown (6). This problem is further exacerbated by siRNA's susceptibility to enzymatic degradation (i.e., RNases) (3). To address these problems, two strategies have been pursued: development of noncharged and nonbiodegradable siRNA surrogates (10) and, more directly, development of delivery vehicles and strategies that would enable or enhance the entry of siRNA itself. Several siRNA delivery technologies have been reported thus far, including direct covalent conjugation of siRNA to lipids, peptides, or to aptamers; and noncovalent complexation of siRNA with polymers, biopolymers, nanotubes, lipid-based vehicles (e.g., lipopolyplexes, stable nucleic acid lipid nanoparticles), cyclodextrin polymer-based nanoparticles, fusion proteins, membrane translocation-modified magnetic nanoparticles, and antibody—protamine conjugates (4, 6, 11–22).

In 2000, we reported an extensive reverse engineering effort directed at the highly cationic HIV-Tat 9-mer peptide (RKKRRQRRR), showing that its ability to enter cells is related to its arginine content and, more specifically, to the number and array of its guanidinium groups (23). This finding led to the design of oligoarginine and guanidinium-rich peptoid cell penetrating agents and, subsequently, a wide range of designed non-peptidic agents, more generally and accurately dubbed molecular transporters, differing in backbone structure but uniformly incorporating the key guanidinium head groups (24). These more synthetically accessible homo-oligomeric transporters performed as well as and often better than the hetero-oligomeric Tat 9-mer in in vitro and in vivo studies. We and others have since shown that these guanidinium-rich molecular transporters can enable or enhance the delivery of a variety of cargos, including small molecules, metals, imaging agents, peptides, plasmids, and proteins across biological barriers, such as cell membranes and the stratum corneum, the latter as part of a clinical trial (24, 25). Recently, we developed an oligomerization strategy that generates unique guanidinium-rich homo-oligocarbonate molecular transporters in an exceptionally step-economical fashion (one to two steps) through a metal-free organocatalytic ring-opening oligomerization reaction (26). With this strategy, the length of the oligomer (degree of polymerization, DP) can be easily tuned by varying the ratio of monomer to initiator in the oligomerization step. The guanidinium-rich oligocarbonate molecular transporters have narrow molecular weight distributions ($M_w/M_n = 1.1 - 1.2$), are reproducibly formed over a range of scales (50 mg to 2.5 g), and, like oligoarginines, readily enter cells. Significantly, this oligomerization strategy can also be deployed to produce co-oligomers of widely varied composition and therefore properties, again in
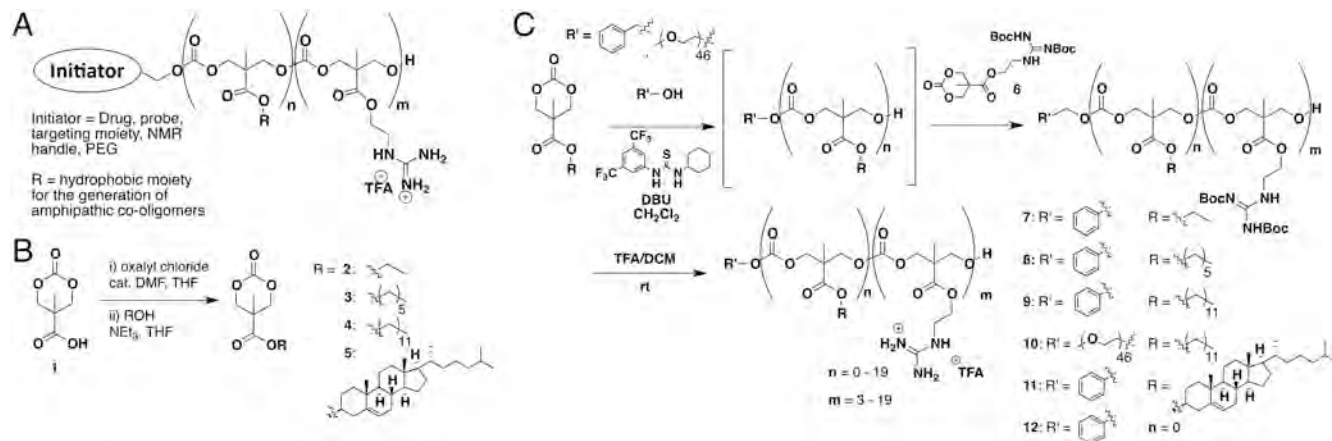
Fig. 1. General structure and synthesis of the guanidinium-rich amphipathic carbonate co-oligomers. (*A*) General structure of the amphipathic carbonate block co-oligomers. (*B*) Synthesis of the hydrophobic monomers from carboxylic acid **1**. (*C*) Amphipathic block co-oligomers were synthesized by organo-catalytic ring opening oligomerization of the monomers, followed by guanidine deprotection with TFA. The scheme depicts the synthesis for a block co-oligomer. Statistical co-oligomers were synthesized by adding both monomers simultaneously at the start of the reaction.

one to two steps through the use of two or more monomers incorporating different side chains (27–29).

We reasoned that the polycationic nature of guanidinium-rich oligocarbonates, if mixed with additional functionality for cell penetration, could be exploited to noncovalently complex and deliver oligonucleotides into cells. More specifically, we hypothesized that amphipathic carbonate co-oligomers, composed of guanidinium-rich side chains to bind siRNA through electrostatic and hydrogen-bonding associations and hydrophobic side chains to facilitate packing and cellular entry (Fig. 1*A*), would serve as effective siRNA complexation and delivery vehicles. Requiring only one to two steps to prepare, the metal-free syntheses of these co-oligomers are uniquely short and facile, thereby allowing one to rapidly synthesize, test, and tune co-oligomers for uptake and offering a distinct advantage over lengthy stepwise synthesis. This co-oligomerization strategy would also be readily amenable to the introduction of targeting elements as the initiator moiety. A further advantage of this approach is that these new carbonate co-oligomers would be biodegradable, a feature that could serve to affect both cargo release and transporter clearance. The method of synthesis, the length of these co-oligomers, the use of the guanidinium group as a cationic complexing moiety and, notably, the biodegradable nature of the oligocarbonate backbone are rare in the siRNA delivery field, and their combination is unique. The distinct advantages offered by this strategy and the speed with which information on siRNA complexation and delivery could be acquired prompted the investigation described herein. We report the study of the synthesis and evaluation of a series of carbonate co-oligomers designed to systematically probe the functionality and factors required for effective complexation, delivery, and release of siRNA.

Results and Discussion

Synthesis of the Guanidinium-Rich Amphipathic Carbonate Co-oligomer Transporters. The initial target set of carbonate co-oligomers was selected to explore the influence of structural variables (e.g., molecular weight, hydrophobicity, ratio of lipid to guanidinium content) on complexation and cellular uptake. As these are the first guanidinium-rich amphipathic co-oligocarbonate transporters to be studied, information on the optimal lipid side chain for siRNA delivery was not known but was expected to be rapidly addressable through the systematic use of monomers incorporating simple, stable and biocompatible lipid side chains (ethyl, hexyl, or dodecyl, Fig. 1*B*: **2–4**). Cholesterol-incorporating monomer **5** was also included to explore the role of more complex polycyclic lipids in both co-oligomer synthesis and performance. Further exemplifying the flexibility and speed of this strategy, the mono-

mers were efficiently accessed by conversion of the cyclic carbonate carboxylic acid **1** to an acid chloride, followed by esterification with selected lipid alcohols (30).

Co-oligomerizations were then conducted using both the requisite hydrophobic monomer and the previously reported guanidine-protected monomer **6** (Fig. 1*C*) (26). A range of DPs (oligomer lengths) was targeted including "short" (Table 1, $m = n =$ approximately 4), "medium" ($m = n =$ approximately 8), and "long" ($m = n =$ approximately 18) co-oligomers. For the hexyl series, co-oligomers with varied lipid to guanidinium ratios were also synthesized to determine how this ratio influences siRNA complexation and delivery. Benzyl alcohol, which serves as a useful handle for characterization purposes, was initially chosen as the initiator. As a further demonstration of the rapid tuning and versatility of this strategy, later iterations incorporated the more complex poly(ethylene glycol) methyl ether (PEG), to explore its effect on complexation and biodistribution. Block co-oligomers were synthesized by mixing the requisite initiator first with each one of the hydrophobic monomers **2–5** in the presence of both the thiourea catalyst (TU) and catalytic base (1,8-diaza-bicycloundec-7-ene, DBU). When the first lipid block had formed, guanidine-protected monomer **6** was added, leading to incorporation of the second protected-guanidine block. Alternatively, statistical co-oligomers were synthesized by using a mixture of the hydrophobic monomer and protected-guanidine monomer at the start of the reaction. Deprotection of the guanidine functionality with trifluoroacetic acid (TFA) in either the block or statistical co-oligomers yielded the desired amphipathic carbonate co-oligomers (Table 1). The synthesized amphipathic carbonate co-oligomers represent variations in overall length (DP = degree of polymerization), initiator moiety, hydrophobic substructure, and hydrophobic to guanidinium ratio, collectively allowing for systematic examination of their ability to noncovalently complex, deliver, and release siRNA.

Characterization of siRNA:Co-oligomer Complexes. As these guanidinium-rich amphipathic carbonate co-oligomers represent a new class of delivery vehicles, our initial focus was to determine whether they would spontaneously form complexes with siRNA. A gel shift assay was used for this purpose. To form the siRNA:co-oligomer complexes, a solution of siRNA in phosphate buffered saline (PBS) was added to a solution of co-oligomer in PBS to obtain siRNA:co-oligomer molar ratios of 1:1, 1:5, 1:10, and 1:25. The resulting solutions were incubated at room temperature to allow time for complex formation (30 min). The complexes were then loaded onto an agarose gel, fractionated, and subsequently stained with ethidium bromide. The

Table 1. Representative synthesized guanidinium-rich amphipathic carbonate co-oligomers. Co-oligomer descriptors refer to the hydrophobic side chain (E = ethyl, H = hexyl, D = dodecyl, Chol = cholesterol) and to the guanidinium group (G) used, followed by numbers that reflect the average number of the respective monomers in the oligomer. The n and m refer to Fig. 1C

Co-oligomer number	Co-oligomer name	n	m	R	Initiator	Type	M_w/M_n*
7a	E:G 5:5	5	5	ethyl	benzyl	block	1.46
7b	E:G 8:9	8	9	ethyl	benzyl	block	1.30
7c	E:G 19:19	19	19	ethyl	benzyl	block	1.42
8a	H:G 4:4	4	4	hexyl	benzyl	block	1.46
8b	H:G 8:9	8	9	hexyl	benzyl	block	1.33
8c	sH:G 9:9	9	9	hexyl	benzyl	statistical	1.26
8d	H:G 10:4	10	4	hexyl	benzyl	block	1.20
8e	H:G 4:10	4	10	hexyl	benzyl	block	1.15
8f	H:G 17:16	17	16	hexyl	benzyl	block	1.35
9a	D:G 4:4	4	4	dodecyl	benzyl	block	1.61
9b	D:G 4.5:5	4.5	5	dodecyl	benzyl	block	1.33
9c	sD:G 4:4	4	4	dodecyl	benzyl	statistical	1.37
9d	D:G 7:7	7	7	dodecyl	benzyl	block	1.47
9e	D:G 18:17	18	17	dodecyl	benzyl	block	1.47
10	PEG-D:G 2.5:3	2.5	3	dodecyl	PEG-2000	block	1.31
11a	Chol:G 3:7	3	7	cholesterol	benzyl	block	1.39
11b	Chol:G 7:7	7	7	cholesterol	benzyl	block	1.37
12	G8	—	8	—	benzyl	block	1.18

*M_w/M_n was determined on the Boc-protected co-oligomer.

ability of each co-oligomer to noncovalently complex with siRNA at a given molar ratio was assessed by the degree to which the migration of the siRNA toward the positive electrode was inhibited (*SI Appendix*, Fig. S1). The highly hydrophobic co-oligomers **8d** and cholesterol-containing **11b** were insoluble in PBS and, therefore, were ineffective in complexing siRNA under the conditions tested. All other co-oligomers with an approximate lipid:guanidinium ratio of 1 or less formed complexes with siRNA.

Gel electrophoresis was also used to assess the hydrolytic stability of the siRNA:co-oligomer complexes. As had been shown previously for the guanidinium-only carbonate oligomers, the carbonate backbone is shelf stable as a solid but, as desired for cargo release after cell entry, it hydrolyses with a half-life of about 8 h in Hepes-buffered saline (pH 7.4, 37 °C) (26). We anticipated that the siRNA:co-oligomer complexes would be similarly stable during cellular entry but subsequently degrade with the release of free siRNA. In a hydrolytic stability assay in the absence of cells, the release of free siRNA could be detected by ethidium bromide staining in a gel shift assay. The siRNA:co-oligomer complexes were incubated for various amounts of time in PBS (pH = 7.4, 37 °C) and then loaded onto a gel and fractionated (*SI Appendix*, Fig. S2). As expected, subsequent staining revealed a stronger uncomplexed siRNA band as the incubation time in PBS increased (8–24 h). While not quantitative, this assay demonstrates that the siRNA:co-oligomer complexes examined in this study generally stay intact during incubation (for at least 4 h), with differences in hydrolytic stability depending on the tunable composition of the co-oligomer. This period is attractive for cell-uptake studies as the complexes are internalized within minutes and before substantial degradation occurs. By 24 h, the complex, regardless of co-oligomer identity, is almost fully degraded. The timing of the siRNA:co-oligomer complex degradation allowed for rapid evaluation of uptake and release in this inaugural study. More generally, this tunable property could also be used to minimize toxicity (see below) or to facilitate local delivery and release, thereby avoiding off-target effects from unintentional systemic exposure.

Dynamic light scattering (DLS) was used to analyze the average diameter of the siRNA:co-oligomer complexes. For these experiments, complexes were formed at the same charge ratio as used in the in vitro siRNA delivery experiments (charge ratio of 4.8/1 +/-) (see below). While all co-oligomers examined by DLS-formed complexes whose sizes could be measured immediately upon mixing with siRNA, some of the co-oligomers, including a guanidinium-only oligomer, formed aggregates that could not be accurately sized and generally were found to be either less effective or ineffective in delivering siRNA (see below). The size of the siRNA:co-oligomer complexes, which is a tunable function of co-oligomer type and siRNA:co-oligomer ratio, ranged in this study from approximately 200 nm in diameter to approximately 1.5 μm (*SI Appendix*, Table S1). These are average sizes and by filtration one can obtain smaller (<200 nm) or larger particle sizes. Over the course of the hour measurement period, some of the co-oligomer complexes increased in size, a phenomenon that has been observed previously in the complexation of polynucleotides with oligoguanidiniums (31). Solutions of only the co-oligomer without siRNA did not form measurable particles at the concentrations used for siRNA:co-oligomer complex formation. Size measurements were not optimized for this study, though they can be further modified by varying the ratio of co-oligomer to siRNA by mixing two distinct co-oligomers with one another before mixing with siRNA, or by utilizing PEG initiated co-oligomers (see below). These results demonstrate that the siRNA:co-oligomer complex size can be tuned by modifying the identity of the amphipathic co-oligomer.

Guanidinium-Rich Amphipathic Carbonate Co-oligomer-Mediated siRNA Delivery In Vitro. The amphipathic carbonate co-oligomers were then screened for their ability to deliver and release siRNA intracellularly. To examine the siRNA:co-oligomer complexes, a dual fluorescent protein reporter assay was used, allowing one protein to be selectively suppressed by its siRNA while the other serves as an internal control. Immortalized human keratinocytes (HaCaTs) were transduced with two distinct lentiviral reporter constructs; one expresses enhanced green fluorescent protein (EGFP), and the other consists of tandem luciferase (Luc2) and tomato fluorescent protein (tdTOM) (Luc2/tdTOM) (32). The siRNA-entitled CBL3 (33) targets the Luc2/tdTOM fusion construct and would therefore reduce, if successfully delivered, the red fluorescent protein expression without affecting the green fluorescent protein expression. The EGFP reporter is valuable as a control for potential nonspecific effects of siRNA administration.

In these experiments, siRNA:co-oligomer complexes were formed by mixing together siRNA and co-oligomer solutions at a positive to negative (+/−) charge ratio of 4.8:1, which was held constant to allow for comparisons of different co-oligomers. The resultant complex was incubated at room temperature for 30 min

and then added to cells along with Dulbecco's modified Eagle medium (DMEM). Cells were incubated with the complex for 4 h, after which the complex was removed and replaced with fresh media, and the cells allowed to incubate for an additional 3 d. Treated cells were analyzed by flow cytometry for both EGFP and tdTOM expression. The coefficient from the division of tdTOM by EGFP was then normalized to untreated cells to determine a percent tdTOM expression that is specific for a reduction in tdTOM relative to EGFP.

All of the amphipathic carbonate block co-oligomers were effective in complexing, delivering, and releasing siRNA, though to varying degrees and with clearly discernible trends, some unanticipated (Fig. 2A). As expected, siRNA itself did not enter cells. Comparison of the ethyl, hexyl, and dodecyl compounds series revealed that, for an overall oligomer length, dodecyl-incorporating co-oligomers outperform their hexyl counterparts, which in turn outperform their ethyl counterparts. Significantly, certain dodecyl-incorporating co-oligomers achieved an average of 86% knockdown of the target protein, with >90% in some experiments. Interestingly, shorter co-oligomers outperform their longer counterparts within each hydrophobic side chain series. The statistical co-oligomers can also effectively deliver siRNA. However, they do not perform consistently relative to their block counterparts (the statistical hexyl co-oligomer **8c** outperforms block co-oligomer **8b**, while the statistical dodecyl co-oligomer **9c** performs similarly to block co-oligomer **9a**). Exchange of the counterion from TFA to chloride does not significantly change siRNA uptake and release. As expected, the delivery into cells of a control siRNA targeting an irrelevant gene using the best performing co-oligomer does not result in reduction of tdTOM expression. In addition, a guanidinium-only homo-oligomer with DP = 8(**12**) also showed no reduction in tdTOM expression, indicating the importance of both hydrophobic and guanidinium groups for effective siRNA delivery. In both untreated and co-oligomer treated cells, the level of expression of green fluorescent protein for a given experiment remained relatively constant, indicating no nonspecific effects on green fluorescent protein expression (*SI Appendix*, Fig. S3). As we were initially interested in the potential of using this technology for as yet unaddressed indications involving intradermal delivery, co-oligomers were screened in the absence of serum. However, dosing siRNA:co-oligomer complex of **9a** in serum-containing media results in effective knockdown (64%), although at a lower level than serum-free media (86%). Efforts to optimize for serum stability were not further investigated in this study.

The amphipathic co-oligomers have batch-to-batch reproducibility. Though **9a** and **9b** have slightly different average molecular weights and different molecular weight distributions, the tdTOM knockdown resulting from the siRNA:co-oligomer complexes of each of these co-oligomers is within error of one another.

A dose response assay was performed for several of the more effective co-oligomers (Fig. 2B: **8a**, **9a**, and **9d**). While both **9a** and **9d** outperform **8a** at the highest dose, **8a** has better activity at lower doses of siRNA:co-oligomer complex.

To further illustrate the specific knockdown at the cellular level, the dual fluorescence reporter HaCaT cells described above were treated with siRNA:co-oligomer complex and then visualized with a fluorescence microscope (Fig. 3). The images show a clear correlation between the flow cytometry results and fluorescent cell images. Untreated HaCaT cells exhibited high levels of both EGFP and tdTOM expression, and all of the amphipathic co-oligomers tested exhibited a selective reduction in tdTOM while maintaining strong EGFP levels. Furthermore, the relative td-TOM knockdown observed for the various amphipathic co-oligomers mirrored the flow cytometry results; **8b**, which had a more moderate level of knockdown, exhibited some observable red fluorescence whereas **8a**, **9a**, and **9d**, all co-oligomers which exhibit >80% tdTOM knockdown by flow cytometry, gave no detectable red fluorescence. Reflecting the potential generality of these findings, the ability of these co-oligomers to deliver a different siRNA for a different target protein [K6a siRNA (34) to target keratin 6a expression] was also confirmed by a reduction in target K6a mRNA levels in HaCaT cells as determined by quantitative reverse transcription PCR (*SI Appendix*, Fig. S4).

Preliminary mechanistic investigations suggest that these complexes are internalized by an endosomal pathway rather than diffusion through the cell membrane or pore formation. Untransfected HaCaT cells, which did not express either of the fluorescent reporter proteins, were treated with amphipathic co-oligomer **9a** that had been complexed with a *Silencer*® FAM™-Labeled Negative Control siRNA (a FITC-labeled siRNA). Cells were then observed with a fluorescence microscope 4 h post treatment and 24 h post treatment (*SI Appendix*, Fig. S5). At 4 h post treatment, punctate green fluorescence was clearly observed, consistent with uptake via an endosomal pathway. By 24 h, the green fluorescence was more diffuse, as would be expected from endosomal escape allowing target knockdown. A small amount of punctate fluorescence remained, implying that future incorporation of an endosomal escape agent into the co-oligomer could further facilitate escape and enable the use of lower siRNA doses (35).
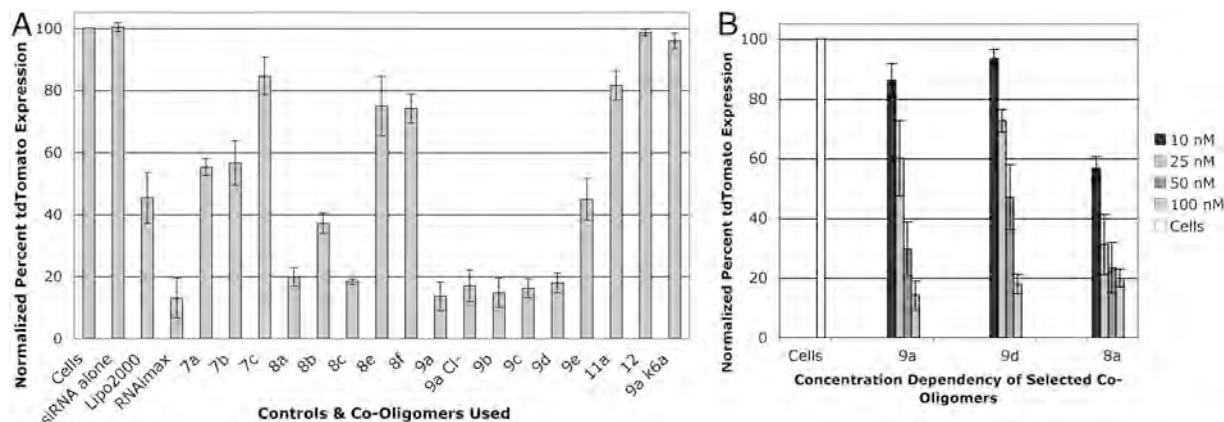

Fig. 2. Reduction in tdTomato (tdTOM) fluorescence normalized to EGFP fluorescence in dual fluorescence reporter HaCaT cells by siRNA:co-oligomer complexes relative to untreated cells, as measured by flow cytometry. Prior to these experiments, cells had been sorted and >90% of the cells express both tdTOM and EGFP. Results are of at least three separate experiments; each condition in triplicate. Error bars indicate SD. (A) Treatment of HaCaT cells with the ethyl, hexyl, and dodecyl siRNA:co-oligomer series. Treatments were 100 nM with respect to siRNA. (B) Dose-dependent reduction in tdTOM fluorescence by several of the best performing co-oligomers.
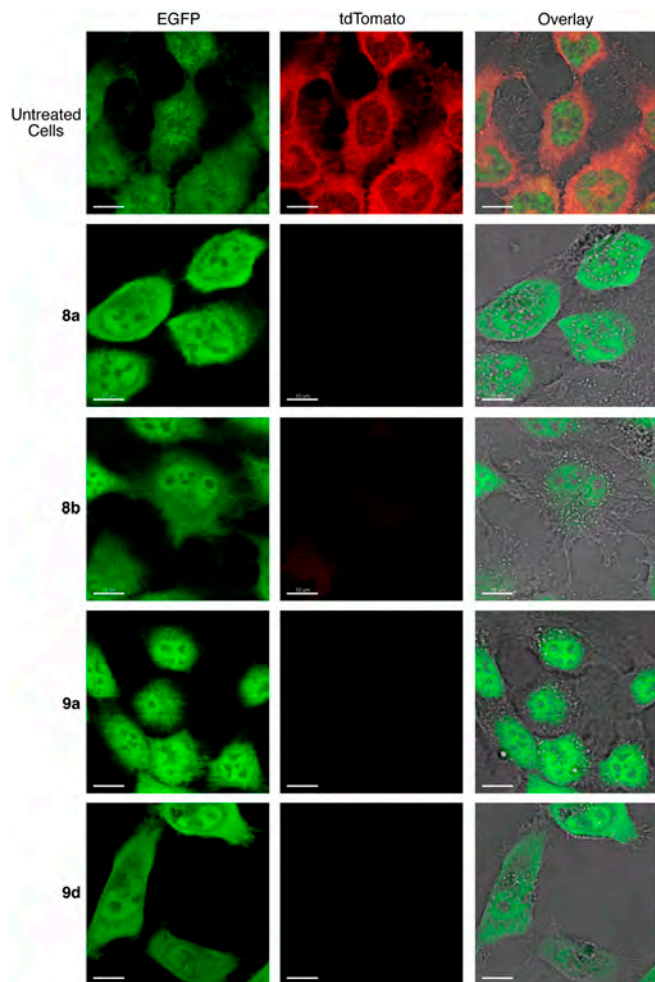
Fig. 3. Fluorescence microscopy of tdTomato (tdTOM) fluorescence and EGFP fluorescence in dual fluorescence reporter HaCaT cells treated with siRNA:co-oligomer complexes. Prior to these experiments, cells had been sorted and >90% of the cells express both tdTOM and EGFP. Treatments were 100 nM with respect to siRNA. The left panel is the green channel only, the middle panel is the red channel only, and the right panel is an overlay of the brightfield image, red channel, and green channel. The scale bar is 10 μm.

Mixtures of Amphipathic Carbonate Co-oligomers for the Delivery of siRNA into HaCaT Cells and Primary Keratinocytes. In addition to the diversity and, thus, tunability that can be rapidly achieved with this step-economical co-oligomer synthesis strategy, including incorporation of various hydrophobic side chains and initiator

moieties, two or more distinct co-oligomers can also be mixed with one another to obtain even greater diversity in siRNA complexation systems and thus in siRNA delivery (or other properties). To demonstrate this option, PEG-initiated co-oligomer **10** was mixed at various molar ratios with **9a**, and then this mixture was combined with siRNA and the resulting complex applied to the dual fluorescence reporter HaCaT cells (Fig. 4A). PEG-initiated co-oligomer **10** exhibits no siRNA delivery ability; however, as the percentage of PEG-initiated **10** relative to **9a** decreases, knockdown increases toward the values obtained for **9a** alone. Significantly, this strategy allows one to tune the size and stability of the complexes as the DLS of the **10** and **9a** complexes with siRNA show a striking decrease in average size and increase in stability by the addition of the PEG-initiated co-oligomer **10**, with all mixtures of **10** and **9a** exhibiting average sizes below 300 nm (Fig. 4B). The incorporation of PEG into these siRNA:co-oligomer complexes, and the resultant control of size and stability are desirable for transitioning to in vivo experiments and other applications (36).

These smaller and more stable siRNA:co-oligomer complexes were then examined for their ability to deliver siRNA and induce knockdown in primary keratinocytes. Primary keratinocytes, which had been transduced with the EGFP and Luc2/tdTOM plasmids, were treated with a siRNA:co-oligomer complex composed of 95:5 **9a**:**10** in a dose-dependent manner, resulting in up to 79% knockdown, with significant knockdown (62%) at only 10 nM (Fig. 4C).

Cytotoxicity of the siRNA:co-oligomer Complexes. To determine the cytotoxicity of the siRNA:co-oligomer complexes, HaCaT cells were treated with siRNA:co-oligomer complexes and then analyzed colorimetrically for mitochondrial reduction of methylthiazolyl-diphenyltetrazolium bromide (MTT) relative to untreated cells (*SI Appendix*, Fig. S6). While this study was designed to explore complexation, uptake, and release and not to minimize toxicity, most of the amphipathic co-oligomer complexes were relatively nontoxic to HaCaT cells at the tested concentrations. Some co-oligomer complexes did display some cytotoxicity but only at the highest concentrations tested (100 nM with respect to siRNA). Importantly, lowering the dose from 100 nM to 50 nM substantially reduces the cytotoxicity of even the most active co-oligomer complexes, conditions which only slightly attenuate the knockdown efficacy. In addition, exchange of the counterion from TFA to chloride reduces cytotoxicity without affecting knockdown efficiency.

Further underscoring the value of biodegradative release, when the siRNA:co-oligomer complexes were pre-incubated in PBS (pH = 7.4, 37 °C) for 24 h (conditions which were shown by gel electrophoresis to result in degradation of the complex), no
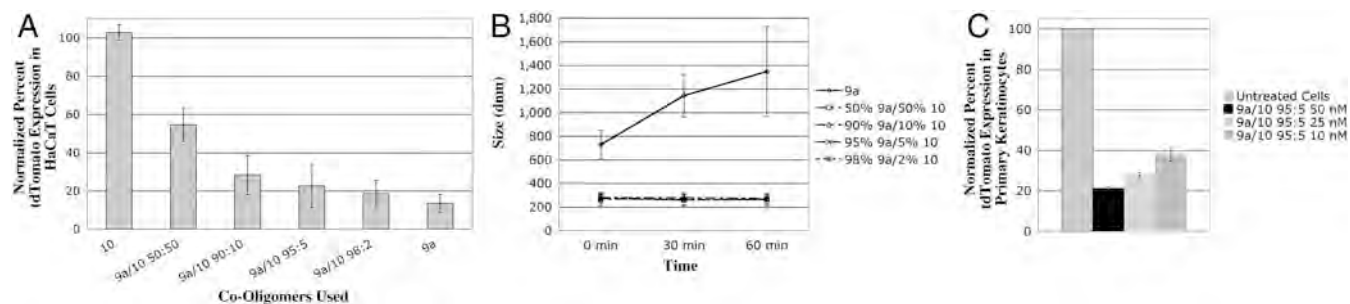
Fig. 4. tdTOM reduction in HaCaT cells and primary keratinocytes by and DLS of siRNA:co-oligomer complexes made from various molar percentage mixtures of **9a** and **10**. The percentages are molar percentages out of a total molar ratio of 1:52.5 siRNA:co-oligomer. (A) Co-oligomers **9a** and **10** were mixed at various molar ratios and then mixed with siRNA. The resulting complexes were applied to cells and analyzed by flow cytometry. Results are of at least three separate experiments; each condition in triplicate. Error bars indicate SD. (B) DLS data on the siRNA:co-oligomer complexes made from mixtures of **9a** and **10** with siRNA. The value shown is the average of three separate trials; error is SD. (C) Primary keratinocytes were treated with siRNA:co-oligomer complexes composed of 95:5 **9a**:**10** in a dose-dependent manner. The value shown is the average of three separate trials. Error is SD.

cytotoxicity was observed. That the amphipathic co-oligomers degrade readily after delivery to nontoxic components could render these particular carriers attractive for local delivery and could lead to improved clearance and reduced toxicity in vivo.

Conclusion

The first members of a new class of block and statistical guanidinium-rich amphipathic carbonate co-oligomers have been designed, synthesized, and evaluated for siRNA delivery. These amphipathic co-oligomers noncovalently complex, deliver, and release siRNA into cells, resulting in up to 90% knockdown (with an average of 86%) of a selected target protein by the best first-generation oligocarbonates evaluated thus far. The organocatalytic oligomerization strategy for accessing these co-oligomers is time and step-economical (one to two steps), metal-free, and readily modified for optimizing delivery. By varying the properties (lipid length) of the monomers used, the properties of the initiator, the relative ratios of the monomers incorporated, and the overall co-oligomer length (DP), the physical properties (e.g., particle size, stability, release rate), and therefore the performance of the co-oligomers, can be tailored for various applications. The performance of the siRNA:co-oligomer complexes can be further controlled by mixing two or more distinct co-oligomers. The biodegradability of these co-oligomers is a distinct advantage of this delivery system and is likely to figure in future in vivo applications. The knowledge derived from this approach could be directly employed in various applications or translated as needed to the preparation of discrete transporters (e.g., amphipathic peptides and peptoids) made through conventional (albeit longer) resin-based or solution-phase synthetic procedures, or to other backbones that can be accessed through organocatalytic oligomerizations. The results of this study, coupled with the ease with which siRNA delivery vectors can be assembled, provide the basis for the broader use of this technology in kit format. The combination of this technology with other delivery techniques [such as microneedles (37) or laser skin ablation (38)] offers further opportunities to achieve therapeutically relevant siRNA delivery. The work reported herein has direct applicability to in vitro siRNA studies and therapies, based on local administration.

Materials and Methods

Additional supplemental figures and tables, information about materials and instrumentation, synthetic procedures, compound characterization data, and experimental details for cellular assays and for the formation and characterization of siRNA:co-oligomer complexes can be found in *SI Appendix*.

1. Leung KM, Whittaker PA (2005) RNA interference: From gene silencing to gene-specific therapeutics. *Pharmacol Ther* 107:222–239.
2. Lares MR, Rossi JJ, Ouellet DL (2010) RNAi and small interfering RNAs in human disease therapeutic applications. *Trends Biotechnol* 28:570–579.
3. Pecot CV, Calin GA, Coleman RL, Lopez-Berestein G, Sood AK (2011) RNA interference in the clinic: Challenges and future directions. *Nat Rev Cancer* 11:59–67.
4. Castanotto D, Rossi JJ (2009) The promises and pitfalls of RNA-interference-based therapeutics. *Nature* 457:426–433.
5. Davidson BL, McCray PB (2011) Current prospects for RNA interference-based therapies. *Nat Rev Genet* 12:329–340.
6. Aagaard L, Rossi JJ (2007) RNAi therapeutics: Principles, prospects, and challenges. *Adv Drug Deliv Rev* 59:75–86.
7. Elbashir SM, et al. (2001) Duplexes of 21-nucleotide RNAs mediate RNA interference in cultured mammalian cells. *Nature* 411:494–498.
8. Burnett JC, Rossi JJ, Tiemann K (2011) Current progress of siRNA/shRNA therapeutics in clinical trials. *Biotechnol J* 6:1130–1146.
9. Leachman SA, et al. (2010) First-in-human mutation-targeted siRNA phase 1b trial of an inherited skin disorder. *Mol Ther* 18:442–446.
10. Karkare S, Bhatnagar D (2006) Promising nucleic acid analogs and mimics: Characteristic features and applications of PNA, LNA, and morpholino. *Appl Microbiol Biotechnol* 71:575–586.
11. Bruno K (2011) Using drug-excipient interactions for siRNA delivery. *Adv Drug Deliv Rev* 63:1210–1226.
12. Hsu T, Mitragotri S (2011) Delivery of siRNA and other macromolecules into skin and cells using a peptide enhancer. *Proc Natl Acad Sci USA* 108:15816–15821.
13. Tan SJ, Kiatwuthinon P, Roh YH, Kahn JS, Luo D (2011) Engineering nanocarriers for siRNA delivery. *Small* 7:841–856.
14. Wang J, Lu Z, Wientjes MG, Au JLS (2010) Delivery of siRNA therapeutics: Barriers and carriers. *AAPS J* 12:492–503.
15. Schroeder A, Levins CG, Cortez C, Langer R, Anderson DG (2009) Lipid-based nanotherapeutics for siRNA delivery. *J Int Med* 267:9–21.
16. Davis ME (2009) The first targeted delivery of siRNA in humans via a self-assembling, cyclodextrin polymer-based nanoparticle: From concept to clinic. *Mol Pharm* 6:659–668.
17. Reischl D, Zimmer A (2009) Drug delivery of siRNA therapeutics: Potentials and limits of nanosystems. *Nanomedicine* 5:8–20.
18. Jeong JH, Mok H, Oh YK, Park TG (2009) siRNA conjugate delivery systems. *Bioconjug Chem* 20:5–14.
19. Liu Z, Tabakman S, Welsher K, Dai H (2009) Carbon nanotubes in biology and medicine: In vitro and in vivo detection, imaging, and drug delivery. *Nano Res* 2:85–120.
20. Eguchi A, et al. (2009) Efficient siRNA delivery into primary cells by peptide transduction-dsRNA binding domain. *Nat Biotechnol* 27:567–571.
21. Medarova Z, Pham W, Farrar C, Petkova V, Moore A (2007) In vivo imaging of siRNA delivery and silencing in tumors. *Nat Med* 13:372–377.
22. Akhtar S, Benter IF (2007) Nonviral delivery of synthetic siRNAs in vivo. *J Clin Invest* 117:3623–3632.
23. Wender PA, et al. (2000) The design, synthesis, and evaluation of molecules that enable or enhance cellular uptake: Peptoid molecular transporter. *Proc Natl Acad Sci USA* 97:13003–13008.
24. Wender PA, Cooley CB, Geihe EG (2012) Beyond cell penetrating peptides: Designed molecular transporters. *Drug Discov Today Technol* 9:e49–e55.
25. Wender PA, Galliher WC, Goun EA, Jones LR, Pillow TH (2008) The design of guanidinium-rich transporters and their internalization mechanisms. *Adv Drug Delivery Rev* 60:452–472.
26. Cooley CB, et al. (2009) Oligocarbonate molecular transporters: Oligomerization-based syntheses and cell-penetrating studies. *J Am Chem Soc* 131:16401–16403.
27. Fukushima K, et al. (2008) Organocatalytic approach to amphiphilic comb-block copolymers capable of stereocomplexation and self-assembly. *Biomacromolecules* 9:3051–3056.
28. Kim SH, et al. (2011) Thermoresponsive nanostructured polycarbonate block copolymers as biodegradable therapeutic delivery carriers. *Biomaterials* 32:5505–5514.
29. Nederberg F, et al. (2011) Biodegradable nanostructures with selective lysis of microbial membranes. *Nat Chem* 3:409–414.
30. Pratt RC, Nederberg F, Waymouth RM, Hedrick JL (2008) Tagging alcohols with cyclic carbonate: A versatile equivalent of (meth)acrylate for ring-opening polymerization. *Chem Commun* 114–116.
31. Choi HS, Kim HH, Yang JM, Shin S (2006) An insight into the gene delivery mechanism of the arginine peptide system: Role of the peptide/DNA complex size. *Biochim Biophys Acta* 1760:1604–1612.
32. Hickerson RP, et al. (2011) Use of self-delivery siRNAs to inhibit gene expression in an organotypic pachyonychia congenital model. *J Invest Dermatol* 131:1037–1044.
33. Gonzalez-Gonzalez E, et al. (2009) siRNA silencing of keratinocyte-specific GFP expression in a transgenic mouse skin model. *Gene Ther* 16:963–972.
34. Smith FJ, et al. (2008) Development of therapeutic siRNAs for pachyonychia congenita. *J Invest Dermatol* 128:50–58.
35. Siprashvili Z, et al. (2003) Gene transfer via reversible plasmid condensation with cysteine-flanked, internally spaced arginine-rich peptides. *Hum Gene Ther* 14:1225–1233.
36. Knop K, Hoogenboom R, Fischer D, Schubert US (2010) Poly(ethylene glycol) in drug delivery: Pros and cons as well as potential alternatives. *Angew Chem Int Ed* 49:6288–6308.
37. Gonzalez-Gonzalez E, et al. (2010) Silencing of reporter gene expression in skin using siRNAs and expression of plasmid DNA delivered by a soluble protrusion array device. *Mol Ther* 18:1667–1674.
38. Prausnitz MR, Langer R (2008) Transdermal drug delivery. *Nat Biotechnol* 26:1261–1268.